Calcium Pyrophosphate Crystal Deposition: The Effect of Monosodium Urate and Apatite Crystals in a Kinetic Study Using a Gelatin Matrix Model

Gretchen S. Mandel
Medical College of Wisconsin

Paul B. Halverson
Clement J. Zablocki VA Medical Center

Neil S. Mandel
St. Luke's Hospital

CALCIUM PYROPHOSPHATE CRYSTAL DEPOSITION:
THE EFFECT OF MONOSODIUM URATE AND APATITE CRYSTALS
IN A KINETIC STUDY USING A GELATIN MATRIX MODEL

Gretchen S. Mandel*, Paul B. Halverson, and Neil S. Mandel

Department of Medicine, Rheumatology Section,
Medical College of Wisconsin,
Research Service, Clement J. Zablocki VA Medical Center,
and St. Luke's Hospital, Milwaukee, Wisconsin.

Abstract

The kinetics of calcium pyrophosphate dihydrate (CPPD) crystal growth was studied by allowing calcium and pyrophosphate (PPi^{-4}) ions to diffuse through a denatured collagen matrix (biological grade gelatin) in the presence of either monosodium urate monohydrate (MSU) or hydroxyapatite (HA) crystals. In this *in vitro* model system, MSU crystals significantly altered the kinetics of PPi^{-4} ionic diffusion through the gelatin matrix by allowing the [PPi^{-4}] gradient to fall off much more rapidly, suggesting an increased level of scavenging of PPi^{-4} ions into crystalline materials. Even more significantly, the presence of MSU crystals markedly influenced the crystal growth morphology of triclinic CPPD, producing that observed *in vivo*. A large number of epitaxially dimensional matches between MSU and triclinic (t) and monoclinic (m) CPPD were identified, suggesting that MSU crystals can epitaxially induce CPPD crystal growth. This finding supports the hypothesis that the association of urate gout and CPPD crystal deposition disease is based on the nucleating potential of MSU crystals for CPPD crystal growth. In contrast, the HA crystal structure did not appear to serve as a nucleating agent for CPPD crystals. However, HA crystals did serve as effective traps for PPi^{-4} ions and their presence led to more stable CPPD crystal growth.

*Address for Correspondence:
Gretchen S. Mandel
Research Service/151
The Clement J. Zablocki VA Medical Center
Milwaukee, WI 53295
Phone number 414-384-2000 ext. 2498

Introduction

Calcium pyrophosphate dihydrate (CPPD) crystal deposition disease has been observed coincident with both urate gout [9,16,18], and basic calcium phosphate (BCP) [4,5,8] crystal deposition disease. Although there is a 2 - 8 % coexistence of pseudogout and gout, this alone does not prove a true association of the two crystal deposition diseases. However, in carefully controlled prospective studies, the prevalence of chondrocalcinosis in patients with gout was 8 out of 138 patients. In age matched normal control patients, and in asymptomatic hyperuricemic patients, the prevalence was 0 of 142 and 1 of 84 patients, respectively. These results do imply a true association of CPPD crystal deposition with gout, but not with hyperuricemia. The nature of this association remains obscure. There may be some common underlying predisposition to both of these two crystal deposition diseases in connective tissues [1]. Alternatively, it has been suggested that urate crystals may act as nucleating substances for CPPD crystal deposition [18].

Several reports have described another mixed crystal deposition disease with the simultaneous clinical appearance of both CPPD and BCP crystals [4,5,8]. No specific clinical syndrome appears to be associated with this disease, although the incidence of mixed crystal disease has been correlated with the severity of osteoarthritis [7]. BCP crystals include hydroxyapatite (HA), carbonate substituted hydroxyapatite (CAP), octacalcium phosphate (OCP), and ß tricalcium phosphate. The crystal structure of CAP is nearly identical to that of HA with approximately a 4% substitution of CO_3 for the hydroxyl ions (and to some extent, the phosphate ions). The structure of OCP is also related to that of HA; it consists of alternating layers, one of which is the HA structure.

We have developed an ionic diffusion model for CPPD crystal deposition in articular cartilage [12]. In this *in vitro* model system, the Ca^{+2} and pyrophosphate (PPi^{-4}) ions must diffuse through a denatured collagen matrix (biological grade gelatin) before they can interact and form CPPD crystals. We also have shown that soluble iron enhances CPPD crystallization and reduces crystal solubilization in this model system [15]. We now report the use of this model system to study the effect of crystalline monosodium urate monohydrate (MSU) and crystalline HA on Ca^{+2} and PPi^{-4} ionic diffusion and on CPPD crystal nucleation and growth.

Neil S. Mandel, Paul B. Halverson, and Gretchen S. Mandel

Materials and Methods

The experimental details for these studies were described previously [12,15]. Gels were prepared, incubated, and harvested as before. All crystals were analyzed by X-ray powder diffraction based on known pyrophosphate structures [10]. Selected crystals were further analyzed by scanning electron microscopy. Calcium concentrations in the gel were determined by atomic absorption analysis and pyrophosphate concentrations were determined using a modified Fiske and SubbaRow method [6]. The ion gradient contour plots were constructed as previously described.

Study I. The effect of excess calcium ions

The experimental details for this study were previously published [12,15]. It serves as the control for Studies II and III, and is therefore included here. Duplicate tubes were harvested at weeks 1, 2, 3, 4, 5, 6, 7, 8, 10, and 12. Each cylinder was sliced into 8 layers, two cm long, and the crystals removed for analysis. Crystals grew in the lower 5 layers which were pooled from the duplicate tubes.

Studies II and III. The effect of MSU and HA crystals in the presence of excess calcium ions

Gels were prepared as described previously [12,15]. Five gelatin partitions were poured. The lowest partition was 15 ml of gelatin containing 10 mM sodium pyrophosphate, the next partition was 5 ml of ion-free gelatin, the next was 20 ml of gelatin plus the MSU or HA crystals, followed by another 5 ml of ion-free gelatin, and finally 15 ml of gelatin containing 50 mM calcium acetate. The MSU crystals were prepared in the size range of 0.5 to 3 μm according to previously published procedures [11] and were used at a concentration of 0.12 mg/ml in a urate saturated gel solution. The HA crystals were prepared by the brushite conversion method [17] and were used at a concentration of 0.133 mg/ml. Hydroxyapatite prepared by this method is usually 6 ± 3 μm in size, contains approximately 2-4 % CO_3, but contains no OCP by X-ray powder diffraction. Gel tubes were harvested at the same time intervals as Study I.

Study IV. The effect of excess pyrophosphate ion

This study was also previously published [12,15], but serves as the control for Studies V and VI, and is therefore repeated here. The gel tubes were harvested on days 4, 6, 7, 10, 12, 14, 19, 26, 33, 40, 47, 55, 69, 97, 125, and 153.

Studies V and VI. The effect of MSU and HA crystals in the presence of excess pyrophosphate ions

Gels were prepared as described previously [12,15]. Five partitions were poured. The lowest partition was 2.5 ml of gelatin containing 50 mM sodium pyrophosphate, the next partition was 2.0 ml of ion-free gelatin, the next was 1.0 ml gelatin plus 0.12 mg/ml of MSU crystals in a urate saturated solution for Study V and 0.133 mg/ml of HA crystals for Study VI, followed by another 2.0 ml of ion-free gelatin, and finally 2.5 ml of gelatin containing 50 mM $CaCl_2$. The gel tubes were harvested as described in Study IV.

Epitaxial Matching

Epitaxial growth is defined as the oriented overgowth of one crystalline lattice onto another. In order for one crystalline lattice to epitaxially grow onto another already formed crystal, the two dimensional crystallographic nets of the two faces, one from each crystal, must be within a few percent of each other so that the crystallographic repeating units will match over extensive areas. In addition, the three dimensional molecular structures must be complimentary so that atoms can form chemically reasonable interactions across the epitaxial face. Using a modified version of the

computer program MATCH1 (3), all reasonable and unique dimensional fits between two dimensional networks found in the three dimensional lattices of both the substrate and the epitaxial structures were calculated. Two dimensional networks were generated by pairing vectors for the origin of one crystallographic unit cell to various lattice points in neighboring unit cells to a maximum distance of 2 nm from the origin. MATCH1 labeled each two dimensional network with the standard crystallographic Miller indices for that family of co-parallel planes. The program recognized and removed vectors which were redundant due to the specific crystallographic point group symmetry in the structure. Two vectors from the substrate structure were paired with two vectors from the epitaxial structure if the vector lengths were within 15% and if the angles between the vector pairs were within 10°. A generalized % misfit was calculated for each dimensional match by summing the percent difference in the two pairs of lattice vectors which defined the contact faces and the percent difference in the angles between the two vectors defining each face. Finally, the network matches were sorted in order of increasing percent misfit. Dimensional matches with a generalized % misfit of <15% were calculated between t-CPPD, m-CPPD, orthorhombic-calcium pyrophosphate tetrahydrate (o-CPPT), MSU, and HA. The number of matching vectors between t-CPPD and MSU was so large that they exceeded the program limits, so dimensional matches beyond 8.8% could not be calculated for this set.

Results

The use of a collagen matrix environment for the diffusion of Ca^{+2} and PPi^{-4} ions leading to the formation of calcium pyrophosphate crystals has proven to be an excellent model for the study of the kinetics of the crystal deposition process. The experimental design has reproducibly produced, at near physiologic conditions, both *in vivo* crystals, t-CPPD and m-CPPD. In addition, the system has produced crystals of o-CPPT, two mixed Ca^{+2}/Na^{+} PPi^{-4} salts, and amorphous calcium pyrophosphate. The crystal types will be denoted t, m, o, C, D, and a respectively; the nomenclature N indicates no crystal growth, and U indicates a small amount of unidentified crystalline material.

The kinetics of the crystal growth process have been analyzed using an ionic gradient map of the changes in $[Ca^{+2}]$ and $[PPi^{-4}]$ as a function of time of incubation, of the crystal type formed, and of the specific position within the tube (Figures 1-6).

Study I

As shown in Figure 1, the control with an excess of Ca^{+2}, the calcium concentrations have been contoured in 1 mM increments using dashed lines originating from the upper left of the plot (the top of the growth tube), and the PPi^{-4} concentrations have been contoured in 1 mM increments in solid lines originating from the right of the plot (the bottom of the tube). The contour levels for both ions were omitted when concentrations exceeded 10 mM. Only the lower 10 cm of gel are shown here since no crystals formed in the original calcium doped partition.

The Ca^{+2} and PPi^{-4} gradients migrated to the center of the tube within one week, interacted at $[Ca^{+2}]$ = 3-7 mM and $[PPi^{-4}]$ = 0.5-2 mM with the formation of crystal o-CPPT. Simultaneously, crystals of m-CPPD also formed in the PPi^{-4} rich partitions. O-CPPT rapidly dissolved at two weeks with a commensurate burst of available PPi^{-4}. Amorphous calcium pyrophosphate formed at 2 weeks at the

Figure 1: The kinetics of CPPD crystal growth in the presence of excess Ca^{+2} (Study I, control for Studies II and III). Both the $[Ca^{+2}]$ and $[PPi^{-4}]$ have been contoured at 1 mM increments, using dashed lines for $[Ca^{+2}]$, and solid lines for $[PPi^{-4}]$. No contours are included for concentrations in excess of 10 mM for clarity. Only the lower 10 cm of gel are shown since no crystals formed in the upper, Ca^{+2} rich layers.
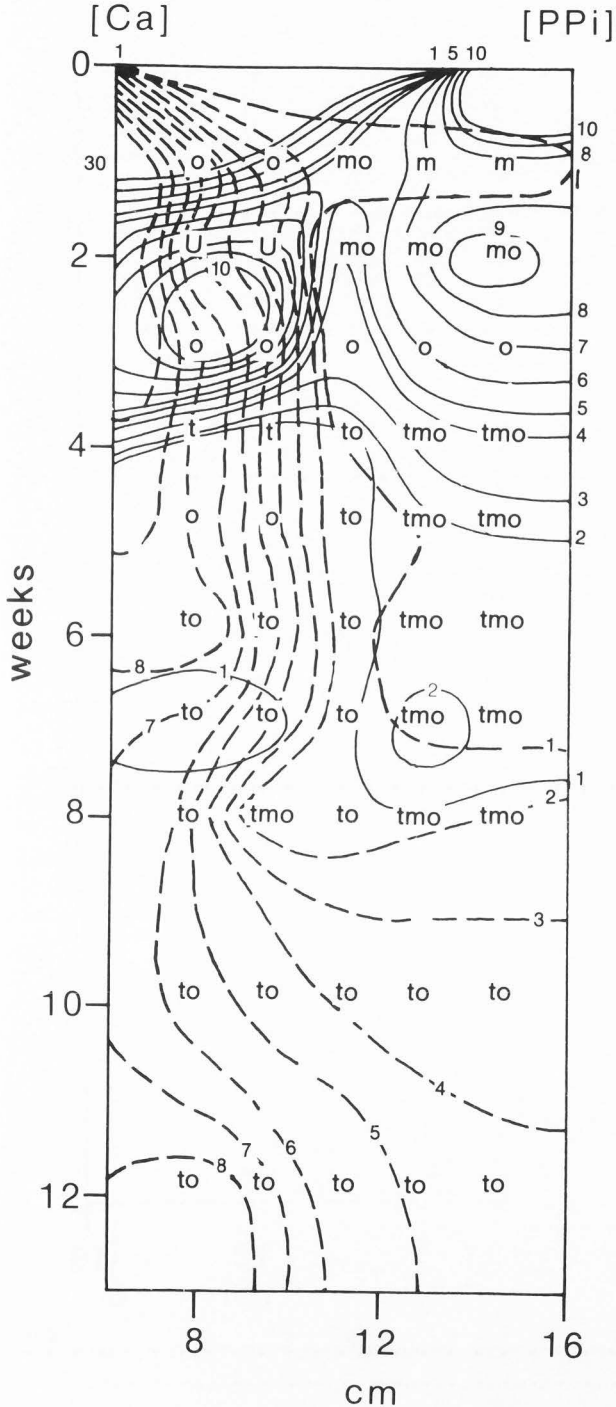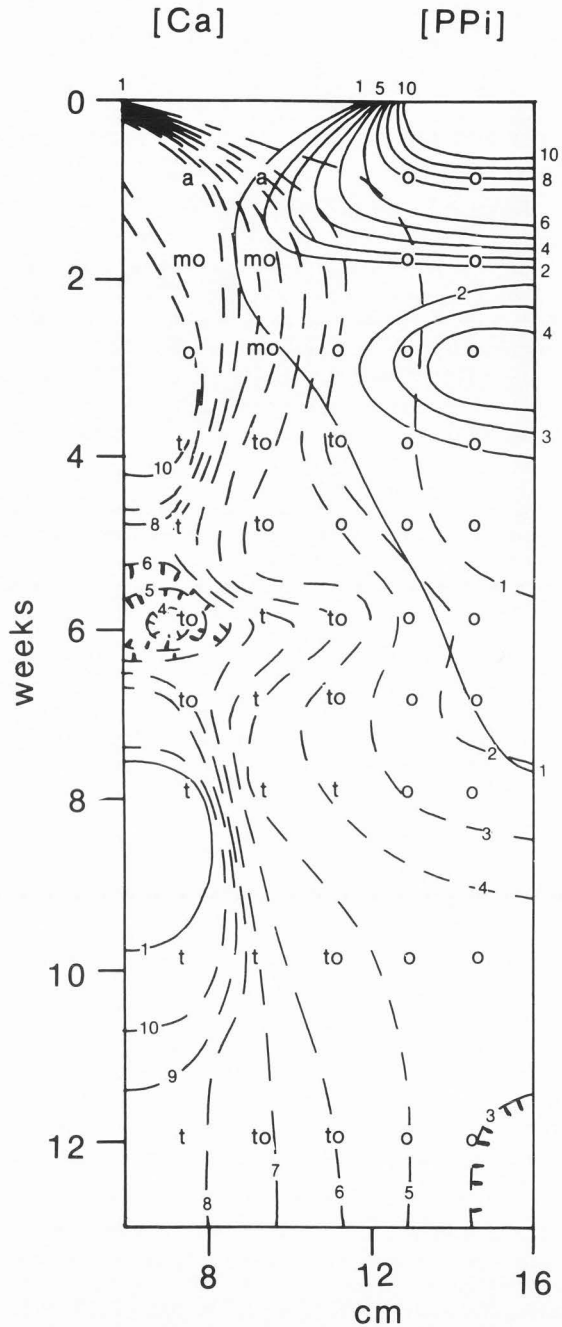
Figure 2: The kinetics of crystal growth showing the effect of MSU crystals in the presence of excess Ca^{+2} (Study II). The crystals were added to the gel layers 4 and 5, which are between 6 - 10 cm. The contours are indicated as described in Figure 1.

high $[Ca^{+2}]$ and $[PPi^{-4}]$ and converted to t-CPPD and o-CPPT at 3-4 weeks. At 8 weeks when the ion concentrations had approached physiologic levels, the crystal types included t-CPPD, m-CPPD, and o-CPPT.

Study II

As shown in Figure 2, the addition of MSU crystals in the presence of excess calcium markedly altered both the ionic gradients and the time of formation and tube position of

the various crystals. There was a rapid fall in [PPi^{-4}] in the PPi^{-4} rich layers. It dropped down to 2 mM within the first 2 weeks, whereas the [PPi^{-4}] had only dropped to 8 - 9 mM in the control in the same time period. With the lower [PPi^{-4}] in the original PPi^{-4} rich layers, only o-CPPT formed in these layers, rather than t-CPPD, m-CPPD, and o-CPPT as in the control. The PPi^{-4} ions migrated into layers 4 and 5 which contained the MSU crystals and crystallized there. At two weeks, m-CPPD and o-CPPT had formed, and by 4 weeks, these crystals dissolved and t-CPPD crystals grew in their place. T-CPPD crystals which formed in these layers remained for the duration of the study.

Study III

As shown in Figure 3, the addition of HA crystals in the presence of excess Ca^{+2} allowed for a rapid diffusion of PPi^{-4} into the HA doped layers. In comparison to the control where there was a drop from 10 to 8 mM PPi^{-4} in the PPi^{-4} rich layers in week 1, and a subsequent dissolution of crystals formed in these layers in week 2, followed by a rapid rise in [PPi^{-4}] in the middle layers in the HA doped system, the [PPi^{-4}] gradient seemed to migrate directly to the HA doped layers and was captured in crystal growth. At week 4, there was a dissolution of some material from the PPi^{-4} rich layers which migrated to the HA doped layers and formed crystals of t-CPPD. These crystals prevailed over the remainder of the time course. No crystals of m-CPPD were ever formed. In part, this may be due to a generally lower [PPi^{-4}] in the PPi^{-4} rich regions which was the primary site of m-CPPD formation in the control.
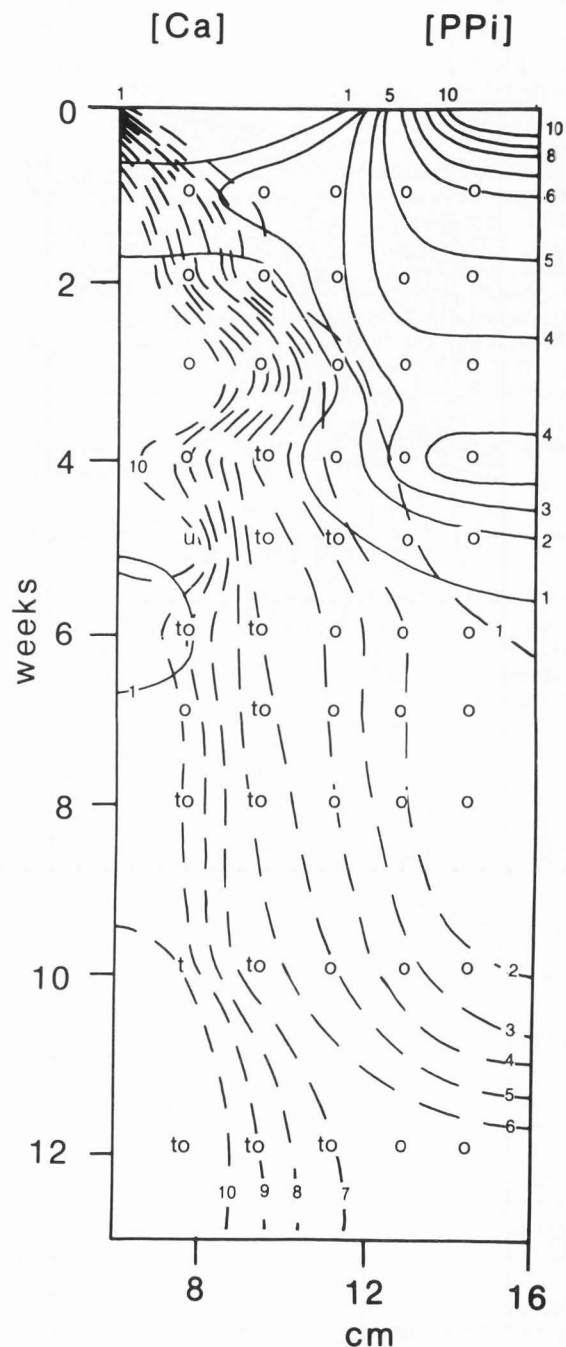
Study IV

As shown in Figure 4, the control with an excess of PPi^{-4}, the kinetic contour map (Figure 4a) of the ionic gradients indicates that the crystal types formed include t-CPPD, m-CPPD, o-CPPT, a, u, C, and D. Figure 4b shows the photographic progression of crystal formation during the 22 weeks of incubation. At high [Ca^{+2}] and low [PPi^{-4}], amorphous formed, was present for 2 weeks, and then transformed to o-CPPT. O-CPPT crystallized in the center of the tube, forming the milky white band seen in Figure 4b and did not dissolve for 6 weeks. The layers towards the PPi^{-4} rich partition produced the two mixed Ca^{+2}/Na^{+} PPi^{-4} salts which prevailed throughout the study. Of note, is that in contrast to Study I where the ionic gradients had not reached equilibrium by 12 weeks, the excess of PPi^{-4} in Study IV appears to have induced ionic equilibrium within the tube at 7 weeks. Also in contrast to Study I, there was relatively little t-CPPD formed in Study IV. Further, there was no crystal growth in the PPi^{-4} rich partitions in the bottom of the tubes or in the calcium rich, upper section of the tubes until the [Ca^{+2}] dropped below 10 mM.
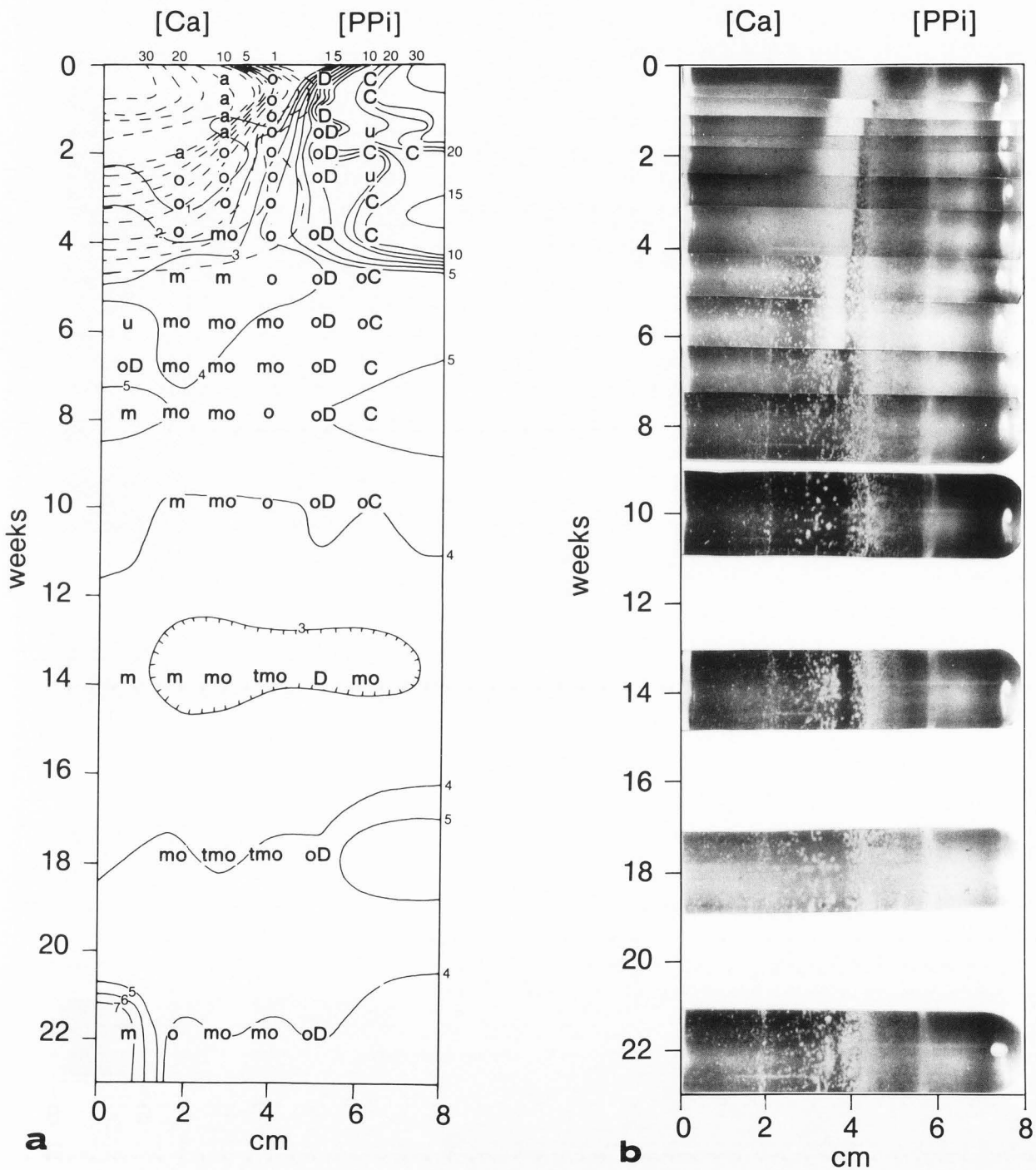
Study V

As shown in Figure 5, the addition to MSU crystals in the presence of excess PPi^{-4} has resulted in the formation of t-CPPD much earlier compared to the control (i.e., formed in the middle layer in 6 weeks compared to 14 weeks in the control). In comparison to the control, there was a more rapid diffusion of the [PPi^{-4}] gradient from the PPi^{-4} layers, but as in the control, the PPi^{-4} gradient passed through the central layers, which in this study contained the MSU crystals. However, this passage of the [PPi^{-4}] gradient through the MSU doped layers resulted in the formation of a broader, more populated, diffuse crystalline band in the center of the tubes which remained 2 weeks longer than in the control (Figure 5b). Further comparison

Figure 3: The kinetics of crystal growth showing the effect of HA crystals in the presence of excess Ca^{+2} (Study III). The crystals were added to the gel layers 4 and 5, which are between 6 - 10 cm. The contours are indicated as described in Figure 1.

Figure 4: The kinetics of CPPD crystal growth in the presence of excess PPi[-4] (Study IV, control for Studies V and VI). In Figure 4a, the contours are as described in Figure 1, except that both [Ca[+2]] and [PPi[-4]] were contoured in 1 mM increments up to 10 mM, above which the increments are 5 mM. The composite photographs monitoring the progressive changes in crystal growth are shown in Figure 4b.

Neil S. Mandel, Paul B. Halverson, and Gretchen S. Mandel

Figure 5: The kinetics of CPPD crystal growth showing the effect of MSU crystals in the presence of excess PPi^{-4} (Study V). In Figure 5a, the contours are as described in Figure 4. The composite photographs monitoring the progressive changes in crystal growth are shown in Figure 5b.

Figure 6: The kinetics of CPPD crystal growth showing the effect of HA crystals in the presence of excess PPi^{-4} (Study VI). In Figure 6a, the contours are as described in Figure 4. The composite photographs monitoring the progressive changes in crystal growth are shown in Figure 6b.
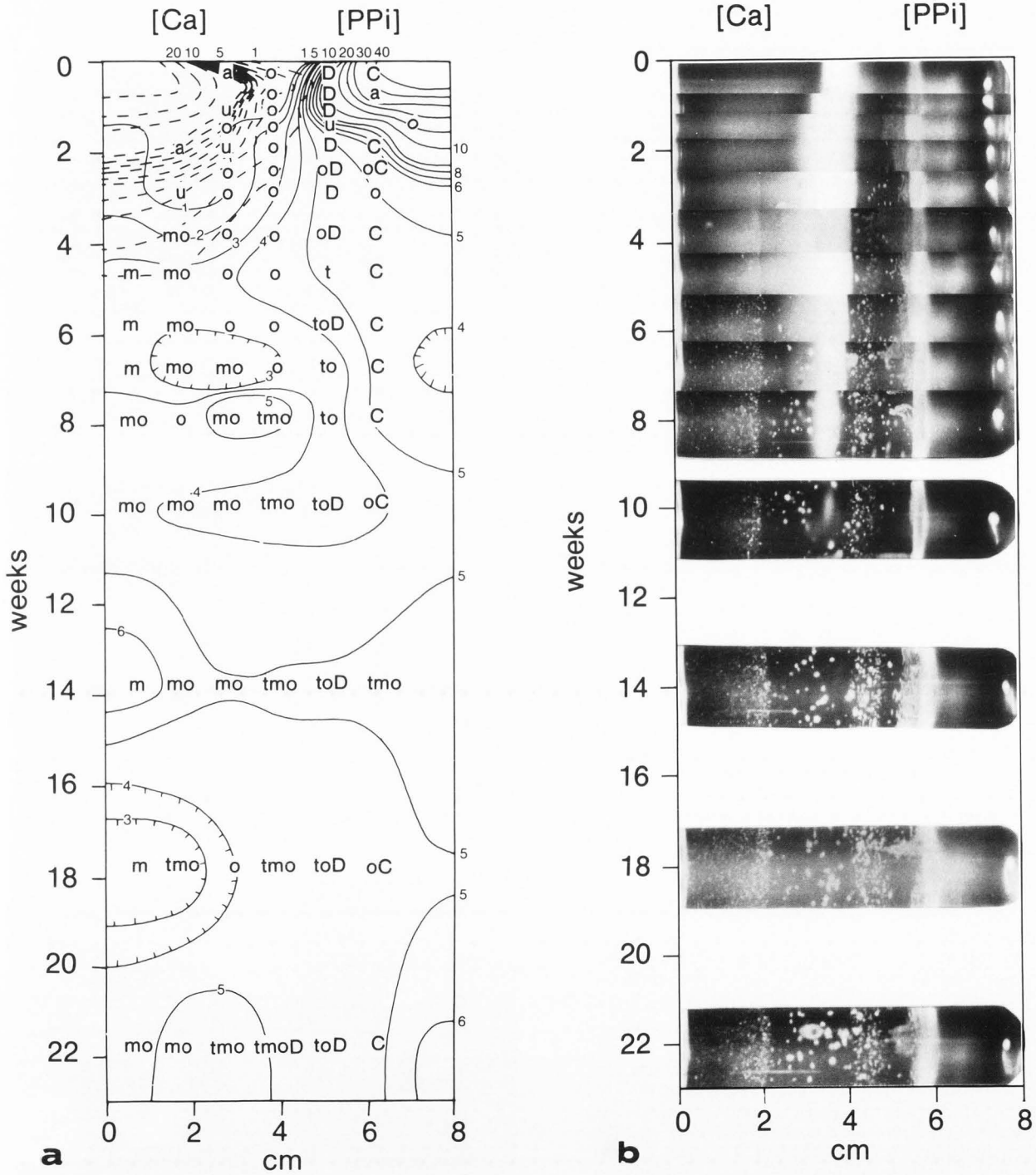
of Figure 4b (control) to Figure 5b, indicates the formation of significantly larger crystals or crystalline aggregates of t-CPPD, m-CPPD, and o-CPPT when the gel was doped with MSU crystals.

Study VI

As shown in Figure 6, the addition of HA crystals in the presence of excess PPi^{-4} has resulted only in subtle differences in the $[PPi^{-4}]$ and $[Ca^{+2}]$ gradients compared to control. It is noteworthy that t-CPPD formed at 5 weeks in layer 5 neighboring the HA doped layers, whereas in the control, t-CPPD never formed in this layer and it took 14 weeks for t-CPPD to initially form in layer 4. In the HA doped layer (layer 4), t-CPPD and m-CPPD formed at 8 weeks, and remained for the remainder of the study. M-CPPD predominated in the Ca^{+2} rich layers, including layer 4 (the HA doped layer). As seen in Figure 6b, the presence of HA crystals led to fewer larger crystalline clusters compared to the control. The diffuse central band disappeared at 8 weeks as in the MSU doped system (Study V).

Morphology

Representative crystal growth morphologies are shown in Figure 7. Crystals of t-CPPD, m-CPPD, and o-CPPT in layer 5, week 8 in the control (Study I) are visible as needles and clumps of needles (Figure 7a). *In vivo* t-CPPD exhibits a distinct prismatic growth morphology [2]. This prismatic morphology was observed in a sample extracted from Study II, layer 4 (MSU doped layer), week 4 (Figure 7b). This sample was pure t-CPPD and every crystal observed by SEM had this morphology. In contrast to the MSU doped samples, the morphology of crystals studied from layer 4, week 8, in the HA doped Study III exhibits identical growth morphology to that observed in the control (Figure 7c).
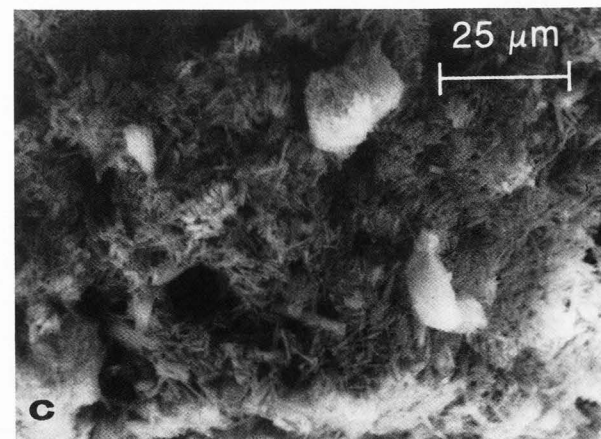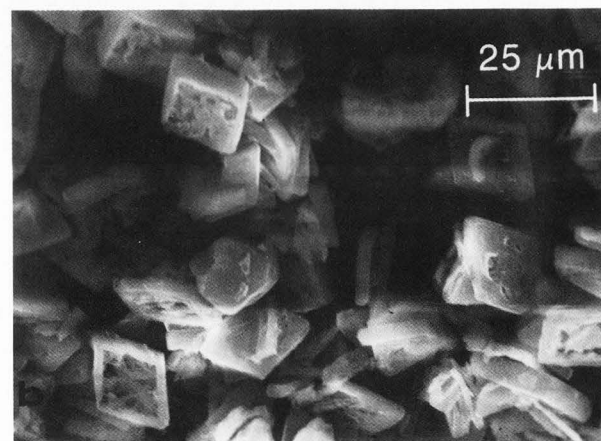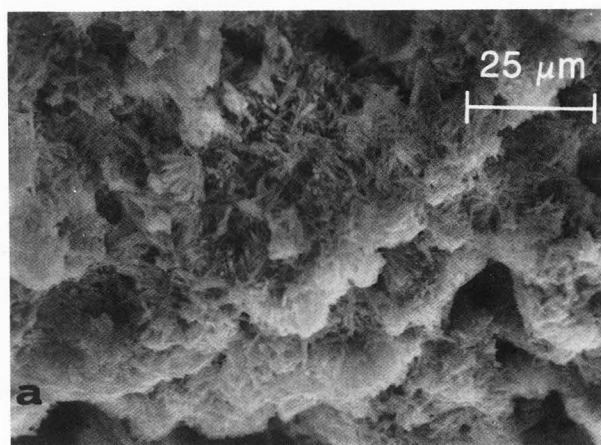
Epitaxial Matching

The potential for epitaxial interactions between the crystals was studied in order to assess whether the significant perturbing effect on t-CPPD growth morphology evidenced by MSU could be due to specific epitaxial nucleation. The number of dimensional matches between the various crystals is shown in Table 1.

Discussion

Previous studies [12,13,15] have shown that Ca^{+2} and PPi^{-4} ionic diffusion through a denatured collagen matrix at physiologic pH could reproducibly yield the two crystals observed *in vivo* in CPPD crystal deposition disease. This study is part of a series investigating the effect that other ions and crystals, which have been observed coincident with CPPD crystal deposition disease, have on CPPD crystal growth kinetics. The current study focuses on the perturbing effects that crystalline MSU and HA have on CPPD crystal growth.

In this *in vitro* model system, MSU crystals significantly altered the kinetics of PPi^{-4} ionic diffusion through the gelatin matrix by allowing the $[PPi^{-4}]$ gradient to fall off much more rapidly, suggesting an increased level of scavenging of PPi^{-4} ions into crystalline materials. In Study II, once t-CPPD formed, it lasted during the entire time course of the study. In other studies [12,15], t-CPPD (as well as m-CPPD and o-CPPT) would form and then dissolve throughout the time course. In Study V, MSU crystals induced the formation of t-CPPD 8 weeks before it crystallized in the control, and induced the formation of larger crystalline clumps. Finally, and most significantly, the presence of MSU crystals produced the distinctive prismatic crystal growth morphology of t-CPPD which is

Figure 7: Scanning electron micrographs of representative samples from Studies I (a), II (b), and III (c). The sample from Study I (a) was formed in the 5th layer, week 8 and contained t-CPPD, m-CPPD, and o-CPPT. The sample from Study II (b) was formed in the 4th layer, week 4 and contained only t-CPPD. The sample from Study III (c) was formed in the 4th layer, week 8 and contained t-CPPD and o-CPPT.

Table 1: The number of dimensional epitaxial matches between the various crystalline dimorphs of calcium pyrophosphate, MSU, and HA. The number of dimensional matches between t-CPPD and MSU was so large that it exceeded the memory capacity of the program.

	< 5%	5% - 10%	10% - 15%
t-CPPD:			
m-CPPD	3	22	83
o-CPPT	0	0	6
MSU	5	56 (to 8.8%)	not done
HA	2	7	18
m-CPPD:			
o-CPPT	1	3	10
MSU	2	19	46
HA	0	6	10
o-CPPT:			
MSU	1	0	6
HA	0	1	3

observed *in vivo* [2]. This morphology was not seen in any of the other samples we investigated.

The epitaxial matches presented in Table 1 suggest that MSU crystals can serve as epitaxial templates for the specific nucleation of CPPD crystals. Table 1 also highlights that t-CPPD and m-CPPD crystals are related crystallographically. This relationship is more fully described elsewhere [14]. MSU also showed potential for epitaxial matches with m-CPPD, which is expected since t-CPPD and m-CPPD are crystallographically related.

In the presence of excess Ca^{+2}, HA crystals only affected the $[PPi^{-4}]$ gradient, in that PPi^{-4} was rapidly attracted to the HA doped layers and was then utilized in crystal formation. In the presence of excess PPi^{-4}, this effect was not observed. In both Studies III and VI, once t-CPPD was formed it never dissolved. In Study VI, there were fewer larger clumps of crystalline material compared to control, indicating that HA favored growth at the expense of nucleation. HA did not exhibit the perturbing effect on CPPD crystal growth morphology observed with MSU.

In conclusion, using this model system, MSU crystals induced t-CPPD crystals to form earlier compared to controls, and also allowed for the formation of larger aggregates of t-CPPD, m-CPPD, and o-CPPT compared to controls. One possible mechanism maybe the epitaxial growth of both t-CPPD and m-CPPD crystals onto MSU crystals. The nucleating potential of MSU crystals for CPPD crystal growth provides one possible explanation of the association of urate gout and CPPD crystal deposition disease. However, MSU crystals have not been identified in the mid-zone of hyaline articular cartilage or deep in meniscus cartilage where CPPD crystals are known to form. Whether or not submicroscopic MSU crystals are present in these areas is presently unknown. In contrast to the effect of MSU crystals, the HA crystal structure did not appear to serve as a nucleating agent for CPPD crystals. However, HA crystals did serve as effective traps for PPi^{-4} ions and their presence led to more stable CPPD crystal growth.

Acknowledgments

References

1. Bjelle OA. (1972). Morphological study of articular cartilage in pyrophosphate arthropathy. Ann Rheum Dis **31**, 449-456.

2. Cameron HU, Fornasier VL, MacNab I. (1975). Pyrophosphate arthropathy. Am J Clin Path **63**, 192-198.

3. Dickens B, Schroeder LW. (1976). Computer programs for structural chemistry: MATCH1 and MATCH2, fortran programs to predict and evaluate mutual orientation of polycrystals. NBS Technical Note 893.

4. Dieppe PA, Crocker PR, Corke CF, Doyle DV, Huskisson EC, Willoughby DA. (1979). Synovial fluid crystals. Q J Med **192**, 533-553.

5. Doyle DV, Dieppe PA, Crocker PR, Ibe K, Willoughby D. (1977). Mixed crystal deposition in an osteoarthritic joint. J Path **123**, 1-5.

6. Fiske CH, SubbaRow Y. (1925). The colorimetric determination of phosphorus. J Biol **66**, 375-403.

7. Gibilisco PA, Schumacher HR, Hollander JL, Soper KA. (1985). Synovial fluid crystals in osteoarthritis. Arthritis Rheum **28**, 511-515.

8. Halverson PB, McCarty DJ. (1979). Identification of hydroxyapatite crystals in synovial fluid. Arthritis Rheum **22**, 389-395.

9. Hollingworth P, Williams PL, Scott JT. (1982). Frequency of chondrocalcinosis of the knees in asymptomatic hyperuricemia and rheumatoid arthritis: A controlled study. Ann Rheum Dis **41**, 344-346.

10. Lehr J, Brown EH, Frazier AW, Smith JP, Thrasher RD. (1967). Crystallographic properties of fertilizer compounds. Chem Eng Bull TVA **6**, 1-166.

11. Mandel NS. (1980). Structural changes in sodium urate crystals on heating. Arthritis Rheum **23**, 772-776.

12. Mandel NS, Mandel GS. (1984). A model for human calcium pyrophosphate crystal deposition disease: Crystallization kinetics in a gelatin matrix. Scanning Electron Microsc.1984; **IV**, 1779-1793.

13. Mandel N, Mandel G. (1984). Nucleation and growth of CPPD crystals and related species in vitro. Calcium in Biological Systems. RP Reuben, G Weiss, JW Putney.(Eds.). New York, Plenum Press, p 711-717.

14. Mandel GS, Renne KM, Kolbach AM, Kaplan WD, Miller JD, Mandel NS. (1988). Calcium pyrophosphate crystal deposition disease: Preparation and characterization of crystals. J Crystal Growth, in press.

15. Mandel GS, Halverson PB, Mandel NS (1988). Calcium pyrophosphate crystal deposition: The effect of soluble iron in a kinetic study using a gelatin matrix model. Scanning Microsc., **2**, 1170-1188.

16. Ryan LM, McCarty DJ. (1985). Calcium pyrophosphate crystal deposition disease; pseudogout; articular chondrocalcinosis. Arthritis and Allied Conditions. DJ McCarty.(Ed.). Philadelphia: Lea and Febiger, p 1547.

17. Spencer M, Grynpas M. (1978). Hydroxyapatite for chromatography: I. Physical and chemical properties of different preparations. J Chrom **166**, 423-434.

18. Stockman A, Darlington LG, Scott JT. (1980). Frequency of chondrocalcinosis of the knees and avascular necrosis of the femoral heads in gout: A controlled study. Ann Rheum Dis **39**, 7-11.

Discussion with Reviewers

R.Z. LeGeros: Were the contours necessary for the conclusions?

Authors: The changes in the contours from the control, depending on the added crystals, form a major basis for the conclusions which we have drawn from these studies.

R.Z. LeGeros: What are the crystals in Figure 7? What crystals correspond to what morphology?

Authors: None of the crystal morphologies in Figure 7a and c could be uniquely identified, so we do not know which crystals are t-CPPD, m-CPPD, or o-CPPT. The crystal morphology observed in Figure 7b is, however, unique to t-CPPD.

R.Tawashi: Figure 7 does not mean very much because these morphologies were obtained at different times and from different layers.

Authors: We have looked at the crystal growth morphologies of many other layers and chosen to publish these because they were representative of the morphologies which we did see at other times and in other layers. The unique duplication of the in vivo crystal growth morphology for t-CPPD observed in the MSU seeded layers is extremely significant since growth morphology is among the most sensitive of all parameters to crystal growth conditions.

R.Tawashi: How do HA crystals serve as effective traps for PPi ions that led to a more stable CPPD crystal growth? It is not clear.

Authors: Comparison of Figures 1 and 3 shows the experimental evidence that the presence of HA crystals resulted in a reduction in the PPi concentration in the gel. The PPi ions have recently been shown to be adsorbed onto HA crystal surfaces at two distinct sites only one of which is involved in the continued growth of HA crystals (Moreno EC, Aoba T, Margolis HC (1987) Pyrophosphate adsoption onto hydroxyapatite and its inhibition of crystal growth. Compend. Contin. Educ. Dent., **Suppl 8**,.S256-S266.). Both sites were presumed to involve the replacement of phosphate ions by PPi ions, particularly at surface defects.

R.Tawashi: What is meant by stable CPPD crystal growth?

Authors: Throughout our studies on the effect of ion concentration [13,14] and various seed crystals and ions [15], we have consistently seen that, in this model system, time is an important parameter. Crystals form, dissolve, and reform. In this particular set of studies, crystals were also formed, but they did not dissolve as frequently as observed in the controls and other seeded studies. Hence, we chose to use the term "stable" to describe this observation.